

# Time delay interferometer channels to suppress gravitational reference sensor disturbances for LISA and Taiji missions

Pengzhan Wu<sup>1</sup> and Peng Xu<sup>1,2,3,\*</sup>

<sup>1</sup>*Institute of Mechanics, Chinese Academy of Sciences, Beijing 100190, China.*

<sup>2</sup>*Lanzhou Center of Theoretical Physics, Lanzhou University, Lanzhou 730000, China.*

<sup>3</sup>*Hangzhou Institute for Advanced Study, University of Chinese Academy of Sciences, Hangzhou 310024, China.*

We reconsidered the anomalies or extra disturbances in gravitational reference sensors (GRS), that would possibly take place in the science operations of the LISA and the LISA-like Taiji missions. The set of time delay interferometer channels  $P_i^{(N)}$  are suggested in this work to sufficiently suppress such GRS position noises of the  $i$ th spacecraft. Given the optimal orbits, we proved that the suppression factor could reach  $10^{-5} \sim 10^{-3}$  in the sensitive band  $0.1 \text{ mHz} \sim 0.05 \text{ Hz}$  for the LISA and Taiji missions. Even for the extreme cases that the GRS noises of one S/C<sub>*i*</sub> have grown to 4 ~ 5 orders of magnitude larger than the designed level, the channel  $P_i^{(N)}$  could still successfully wipe out the extra noises and retain the expected sensitivity level. With this approach, the feasibility of the LISA and Taiji missions could be improved, and the risks relate to GRS systems could be significantly reduced.

## I. INTRODUCTION

The first detection of gravitational wave (GW) in 2015 by Adv-LIGO [1–4], together with the subsequent observations by the LIGO-VIRGO collaboration in the following years, had gradually open the new era of the gravitational wave astronomy. To enclose the exciting sources in the millihertz band, the pioneering mission concept of the Laser Interferometer Space Antenna (LISA) was proposed in 1993 as a “cornerstone mission” to the ESA’s “Horizon 2000 plus” program [5–7]. Today, LISA, as the most fully-fledged mission concept under development, had been selected as the ESA’s L3 (Large) mission that scheduled to be launched in the 2030s [8].

Following the mission concept of ALIA [9], China had started her own pursuit of GW detection in space since 2008. Then, under the collaboration between the Max Planck Institute for Gravitational physics and the Chinese Academy of Sciences (CAS), the first Chinese mission concept was proposed in 2011 [10] and afterward a descoped and more conservative design was made in 2015 [11, 12]. Based on the preliminary studies, and also encouraged by the breakthroughs made by both the LIGO and the LISA PathFinder (LPF) mission [13–15], the “Taiji Program in Space” was released by the CAS in 2016 and the journey to China’s space-borne GW observatory had officially set forth [16–19]. Taiji belongs to the LISA-like missions, and according to its road map [17, 18], it is expected that the science operations of LISA and Taiji may overlap in the 2030s. Studies of the space antenna network that formed by these two missions has now aroused more interest [20–24].

For both the LISA and Taiji missions, the expected sources, especially SMBH mergers and EMRIs, produce GW signals that last for months or even years within

the sensitive bandwidth. To precisely measure the related parameters and infer the physical properties of such sources, continues measurements without disruptions in the data streams are normally required. This imposes strong challenges on the long-term stability and robustness of both the high precision payloads and ultra-stable satellite platforms. According to the designs of the LISA and Taiji missions, the foreseeable disruptions in science measurements may come from the scheduled maintenances and unexpected instrument anomalies. Scheduled maintenances could cause large and even continuous disturbances of satellite platforms and affect heavily the performances of the key payloads, such as the lasers, interferometers and especially the gravitational reference sensors (GRS). On the other hand, based on the experiences of the LPF [13, 14, 25], GRACE [26] and Taiji-1 [27] missions, the GRS or accelerometer systems would also be affected by random transient anomalies. It is then conservative to expect that the aforementioned GRS anomalies would take place in the science operations of both LISA and Taiji missions, which would affect the GW signals detection and parameter estimations in science data analysis. For even more extreme cases, it would be possible that one of the satellites could not retain its ultra-stable and clean state for a rather long time due to some abnormal conditions, therefore the performances of one or even both of the GRSs onboard such satellite would be seriously affected and result into unwanted long-term data gaps.

In early studies, Pollack [28], Carre and Porter [29] had analyzed the effects of simple data gap models on monochromatic signals detection and parameter estimations. With the important anomalies found in LPF’s observations [25, 30], the consequences of realistic data anomalies, such as non-stationary noises, glitches, gaps and etc., have been taken seriously and drawn more attentions in recent studies [31–33].

In this work, we reconsider the issues caused by the GRS data anomalies and continuous disturbances. Dif-

---

\* xupeng@imech.ac.cn

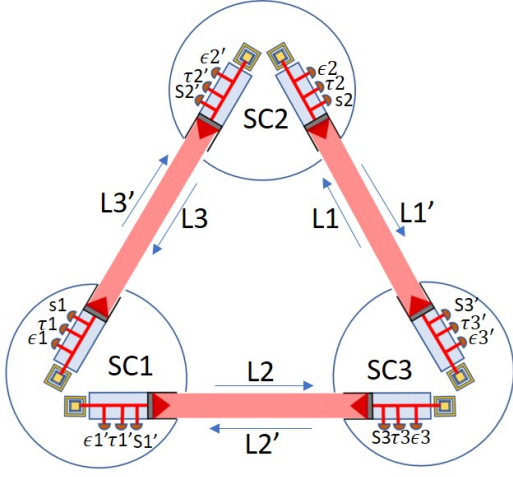


Figure 1: The measurements scheme for the LISA and the LISA-like Taiji missions.

ferent from noises modelings and subtractions from the data in pre-processing, or carrying parameters estimations with data gaps in science processing, we suggest a novel approach to sufficiently suppress the noises from GRS systems by means of the set of “position noise suppressing” time-delay interferometer (TDI) channels.

## II. MEASUREMENT SCHEME AND TIME DELAY INTERFEROMETRY

We introduce here the measurement scheme for the LISA and the LISA-like Taiji missions, and also the notations used in following sections. For LISA and Taiji, the so-called “split interferometer” is adopted, see [8, 34, 35] for detailed discussions. For each one-way inter-satellite interferometry, the measurement is divided into three parts, that of the inter-satellite science interferometer  $s(t)$  that links the optical benches (OB) between the two spacecrafts (S/C), and the two local test mass (TM) interferometers  $\varepsilon(t)$  that each measures the distance between the local TM of the GRS and the OB. Together with the reference (backlink) interferometers  $\tau(t)$  between the two local lasers of the same S/C, the complete one-way inter-satellite laser ranging  $\eta(t)$  that connecting the free-falling TMs can be formed. For clarity, we ignore the phase locking scheme and discuss here the six sets of one-way measurements. Please see Fig. 1 for the labels of constellation arms, S/Cs, OBs, and the aforementioned interferometers.

For each OB, we will have three interferometers, that  $s_i(t)$ ,  $\varepsilon_i(t)$  and  $\tau_i(t)$ . Take the OB<sub>1</sub> of S/C<sub>1</sub> as an example, the readouts of the interferometers, in terms of relative frequency variations  $\delta\nu/\nu_0$  of the carrier, can be

written down as

$$s_1(t) = \theta_1^s(t)[H_1(t) + D_3 p_{2'}(t) - p_1(t) - \vec{n}_3(t) \cdot D_3 \frac{d\vec{\Delta}_{2'}(t)}{cdt} - \vec{n}_{3'}(t) \cdot \frac{d\vec{\Delta}_1(t)}{cdt}] + N_1^s(t), \quad (1)$$

$$\varepsilon_1(t) = \theta_1^\varepsilon(t)[p_{1'}(t) - p_1(t) + 2\vec{n}_{3'}(t) \cdot (\frac{d\vec{\Delta}_1(t)}{cdt} - \frac{d\vec{\delta}_1(t)}{cdt}) + \mu_{1'}(t)] + N_1^\varepsilon(t), \quad (2)$$

$$\tau_1(t) = \theta_1^\tau(t)[p_{1'}(t) - p_1(t) + \mu_{1'}(t)] + N_1^\tau(t). \quad (3)$$

Here,  $p_i$  denotes the fractional frequency noise from the  $i$ th laser,  $\vec{\Delta}_i$ ,  $\vec{\delta}_i$  the position noises from the  $i$ th optical bench and TM, and  $\mu_i$  the path noise caused by the optical fiber in the backlink interferometer. Frequency modulations caused by GWs  $H_i$  are encoded in the inter-satellite signals  $s_i(t)$  of the science interferometer. The time delay operator  $D_i f(t) = f(t - L_i/c)$ , and  $\vec{n}_i$  denotes the unit vector of the inter-satellite link. The sign function  $\theta_i$  is defined by the frequency difference of the beating lasers, and  $N_i$  contains the rest noises such as the clock noise, thermo-mechanical noise, electronic noise and etc.. The inter-satellite TM-to-TM one-way ranging then reads

$$\eta_1(t) = \theta_1^s(t)s_1(t) + \frac{\theta_1^\tau(t)(\varepsilon_1(t) - \tau_1(t))}{2} + \frac{\theta_{2'}^\tau(t)D_3(\varepsilon_{2'}(t) - \tau_{2'}(t))}{2} + \frac{\theta_{2'}^\tau(t)D_3(\tau_{2'}(t) - \tau_2(t))}{2} \quad (4)$$

where the position noises from the OBs  $\Delta_1$  and  $\Delta_{2'}$  are cancelled out. The interferometric readouts of OB<sub>1'</sub> can be written down in the same way according to Fig. 1, and the readouts for S/C<sub>2</sub> and S/C<sub>3</sub> can be obtained with the permutation rules of indices “1 → 2 → 3 → 1”, see [35–37] for detailed discussions.

The one-way ranging data  $\eta(t)$  is dominated by laser frequency noise  $p(t)$ , which is the key noises of the science measurements of LISA-like missions. To resolve this problem and sufficiently remove the laser frequency noises, Armstrong, Estabrook and Tinto [38, 39], Ni and collaborators [40] in late 1990s had suggested employing the TDI method to form equal arm interferometers with the aforementioned 6 one-way rangings. This is equivalent to find solutions of the following algebra equations for the delay operators

$$\sum_{i=1,2,3,1',2',3'} F^i(D_1, D_2, D_3, D_{1'}, D_{2'}, D_{3'}) \eta_i = h(H_1, H_2, H_3, H_{1'}, H_{2'}, H_{3'}) + \text{secondary noises},$$

where  $F^i$  and  $h$  are polynomials functions. One also notices that in general cases the delay operators may not be communicative, that  $D_i D_j \neq D_j D_i$ .

The TDI method would constitute the core of the data pre-processing procedure of the missions. One could consult the comprehensive review by Tinto and Dhurandhar [36], and also the theses [35, 37, 41, 42] for details. It is natural to re-consider the GRS noise suppression within the TDI framework.

### III. DISTURBANCES FROM GRS

GRSs are of the key payloads for LISA-like missions. The TMs suspended inside each GRS can be viewed as the end mirrors for the inter-satellite interferometers, see Fig. 1. Any disturbances of their free-falling states will produce noises that pollute the science measurements.

For LISA and Taiji, the residual acceleration noises of the TMs along their sensitive axes are designed to be better than  $3 \times 10^{-15} \text{ m/s}^2/\text{Hz}^{1/2}$  in the millihertz band [8, 17, 18, 43]. This means that the GRS systems are extremely sensitive to slight disturbances from

payloads or platforms. For example, the accelerometers of GRACE responded to events like the foil thermal effects and heating system switches, and produced transient phantom signals which affected about 30% of the measured data [26, 44]. To obtain a better performance, it is suggested to model and subtract such transients from the data in the pre-processing procedure [45–47]. For LPF, unexpected transient events or glitches were found to happen rather frequently (about 0.7 times per day) during the science runs [25, 30]. The requirement of LISA free-fall performance ( $\sim 3 \times 10^{-15} \text{ m/s}^2/\text{Hz}^{1/2}$ ) had been successfully confirmed only after such glitches and other modeled noises were precisely removed in the data [14, 25].

For the Taiji-1 mission [27, 48], the GRS was also found to respond to small vibrations like thruster events, see Fig. 2a. Especially, during the science run, we also investigated how the GRS responded to large and continuous

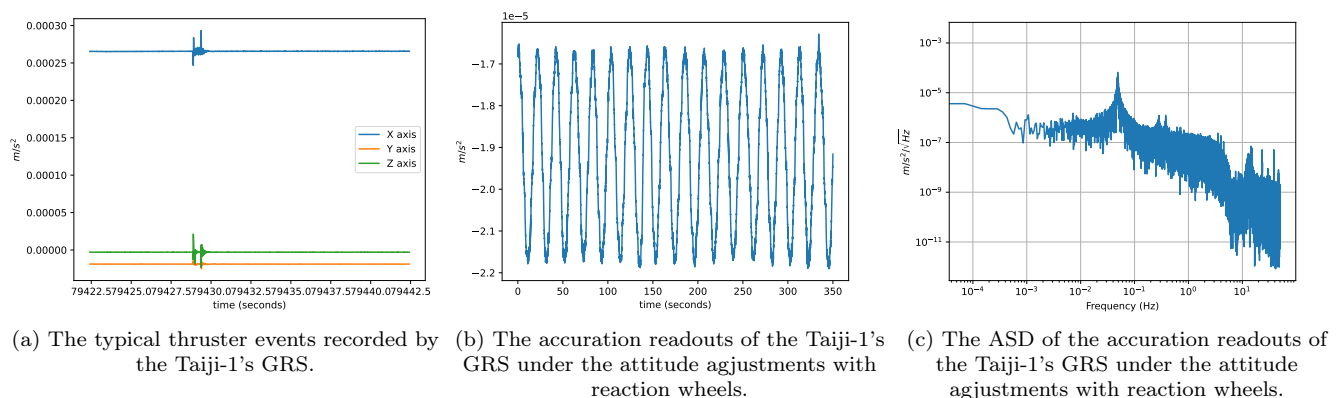


Figure 2: The typical responses of the Taiji-1's GRS to small vibrations and continuous disturbances.

disturbances from the satellite platform, such as vibrations caused by reaction wheels during attitude adjustments [49–52]. In Fig. 2b and 2c, one sees the  $\sim 20\text{s}$  period signal in the time series and the ASD (amplitude spectrum density) plots, which was produced by the aliasing of the  $\sim 6000 \text{ Hz}$  vibrations due to reaction wheels. The overall noise level of the GRS was also lifted by such maneuvers compared to the case of nominal science runs.

Given the valuable experiences from these missions, the performances of the GRSs for the LISA and Taiji missions may inevitably be affected by the unexpected anomalies and scheduled maintenances. Here we study the *real* transient glitches and continuous disturbances exerted by the TMs, that they produce deviation accelerations of the TMs relative to the local free-falling inertial frames. They will be picked up by the TM interferometers but not the science interferometers, and can not be canceled out in the combinations  $\eta(t)$ . Henceforth, such disturbances in GRS will propagate through the TDI channels [31, 53–55] and affect GW signal detections and parameter estimations in science data analysis, which needs to be carefully accounted and resolved in the data pre-processing stage. Especially, for continuous disturbances from telecommunication antennas adjust-

ments, re-calibration maneuvers etc., the couplings between the TM and environment may cause the growth of its acceleration noises over the entire measurement band. This affects the performances of the two GRSs onboard the same S/C under maintenance, therefore will pollute or even break down the measurement arms and result into the unwanted long-term data gaps.

Without loss of generality, in the following section we model the possible two classes of anomalies in GRS measurements based on the previous discussion. For transient glitches, according to LPF's observations, the most frequent glitches are of the fast rise and exponential decay type and the sine-Gaussian type. We model such transients following the important work [25, 30], see simulations in Fig. 4a. According to the Taiji-1's experiments, we could model the continuous disturbances in

GRS caused by satellite maintenances as the fast growths and gradually decays of the position noise at the starts and the ends of the maneuvers respectively, see Fig. 4b. Even though in real measurements the data anomalies could be much more complicated, the two models could meet the requirement for testing the new noise suppression algorithm in this work.

#### IV. SUPPRESSING GRS DISTURBANCES IN TDI CHANNELS

##### A. Suppressing GRS disturbances

Suppose that due to some abnormal conditions or continuous disturbances of one of the satellites, say S/C<sub>2</sub>, the performances of one or both of the GRSs on-board this satellite is seriously affected. In this condition, the TM interferometers  $\varepsilon_2(t)$  and  $\varepsilon_{2'}(t)$  may contain many large spikes or glitches, and the variances of the position noises  $\vec{\delta}_2(t)$  and  $\vec{\delta}_{2'}(t)$  may become much worse relative to their nominal level. In terms of the one-way measurement, the data from the following four measurement links  $\eta_1(t)$ ,  $\eta_{1'}(t)$ ,  $\eta_3(t)$ ,  $\eta_{3'}(t)$  of the two arms  $L_1$ ,  $L_3$  will be polluted by the extra noisy terms  $\vec{\delta}_2^E$  and  $\vec{\delta}_{2'}^E$ , see Eq. 4. All the conventional TDI combinations, such as Michelson types, Sagnac types, the link failure surviving combinations and the optimal sensitivity combinations, have to include links among these four, which could not give rise to data products retaining the expected noise level ( $\sim 6\mu\text{rad}/\text{Hz}^{1/2}$ ) and being free of the extra position noises  $\vec{\delta}_2^E$  and  $\vec{\delta}_{2'}^E$ , see Fig 5a and 5b.

To resolve this problem, we introduce here the “position noise suppressing” TDI channels  $P_i$ , where  $i = 1, 2, 3$  is the label of the S/C. For simplicity, let's first focus on the 1st-generation TDI combinations. Continuing with the foregoing example, we consider the Sagnac combinations started with S/C<sub>1</sub>, and S/C<sub>3</sub> [36, 56]

$$\begin{aligned}\alpha &= (D_{1'}D_{2'}\eta_{2'} + D_{2'}\eta_{3'} + \eta_{1'}) - (D_1D_3\eta_3 + D_3\eta_2 + \eta_1), \\ \gamma &= (D_{3'}D_{1'}\eta_{1'} + D_{1'}\eta_{2'} + \eta_{3'}) - (D_3D_2\eta_2 + D_2\eta_1 + \eta_3).\end{aligned}$$

For the  $\alpha$  combination with noisy terms  $\vec{\delta}_2^E$  and  $\vec{\delta}_{2'}^E$ , one could neglect for clarity all the normal noise terms not related to  $\vec{\delta}_2^E$  and  $\vec{\delta}_{2'}^E$ , since they remain the same as in the original expression of  $\alpha$ , therefore, in terms of fractional frequency variations, we have

$$\begin{aligned}\alpha &= D_{2'}D_{1'}[\vec{n}_{1'}(t) \cdot \frac{d\vec{\delta}_{2'}^E(t)}{cdt}] - D_{2'}D_{1'}[\vec{n}_3(t) \cdot \frac{d\vec{\delta}_{2'}^E(t)}{cdt}] \\ &\quad + D_3[\vec{n}_3(t) \cdot \frac{d\vec{\delta}_{2'}^E(t)}{cdt}] + D_3[\vec{n}_{1'}(t) \cdot \frac{d\vec{\delta}_2^E(t)}{cdt}] \\ &\quad + N.T.,\end{aligned}\tag{5}$$

where  $N.T.$  stands for all the other normal noise terms.

In the same way,  $\gamma$  reads

$$\begin{aligned}\gamma &= -D_{1'}[\vec{n}_3(t) \cdot \frac{d\vec{\delta}_2^E(t)}{cdt}] - D_{1'}[\vec{n}_{1'}(t) \cdot \frac{d\vec{\delta}_2^E(t)}{cdt}] \\ &\quad + D_3D_2[\vec{n}_{1'}(t) \cdot \frac{d\vec{\delta}_2^E(t)}{cdt}] + D_3D_2[\vec{n}_3(t) \cdot \frac{d\vec{\delta}_{2'}^E(t)}{cdt}] \\ &\quad + N.T..\end{aligned}\tag{6}$$

As expected, the GRS disturbances  $\vec{\delta}_2^E$  and  $\vec{\delta}_{2'}^E$  from S/C<sub>2</sub> remain within the TDI-filtered data, see simulations in Fig. 5a and 5b.

While, the crucial observation is that, in both the  $\alpha$  and  $\gamma$  combinations, the corresponding extra noisy terms have the same forms and almost the same delay times. For example, the clockwise loop of  $\gamma$  has the GRS extra noise terms from  $TM_2$  and  $TM_{2'}$  with delay time of one arm  $L_{1'}/c$ , while the counter-clockwise loop of  $\alpha$  contains the same noise terms with opposite signs and almost the same one arm delay time  $L_3/c$ . Adding the two TDI combinations will then produce the differences of the extra GRS noise terms with delay time of one arm. The same is for the extra GRS noise terms with delay time of two arms.

We then define the position noise suppressing channel  $P_2$  for node 2 (or S/C<sub>2</sub>)

$$\begin{aligned}P_2 &= \frac{1}{\sqrt{2}}(\alpha + \gamma) \\ &= \frac{1}{\sqrt{2}} \left( D_3[\vec{n}_3(t) \cdot \frac{d\vec{\delta}_{2'}^E(t)}{cdt}] - D_{1'}[\vec{n}_3(t) \cdot \frac{d\vec{\delta}_{2'}^E(t)}{cdt}] \right) \\ &\quad + \frac{1}{\sqrt{2}} \left( D_3[\vec{n}_{1'}(t) \cdot \frac{d\vec{\delta}_2^E(t)}{cdt}] - D_{1'}[\vec{n}_{1'}(t) \cdot \frac{d\vec{\delta}_2^E(t)}{cdt}] \right) \\ &\quad + \frac{1}{\sqrt{2}} \left( D_3D_2[\vec{n}_{1'}(t) \cdot \frac{d\vec{\delta}_2^E(t)}{cdt}] - D_{2'}D_{1'}[\vec{n}_{1'}(t) \cdot \frac{d\vec{\delta}_2^E(t)}{cdt}] \right) \\ &\quad + \frac{1}{\sqrt{2}} \left( D_3D_2[\vec{n}_3(t) \cdot \frac{d\vec{\delta}_{2'}^E(t)}{cdt}] - D_{2'}D_{1'}[\vec{n}_3(t) \cdot \frac{d\vec{\delta}_{2'}^E(t)}{cdt}] \right) \\ &\quad + \frac{1}{\sqrt{2}}N.T.\end{aligned}\tag{7}$$

Let us denote the armlength difference between  $L_i$  and  $L_j$  as  $\Delta L_{ij}$ . According to the optimized orbits of LISA and Taiji, the maximum armlength variations are  $\leq 1.2 \times 10^4 \text{ km}$ , relative velocities  $\leq 6 \text{ m/s}$  and therefore the armlength difference is  $\leq 2.4 \times 10^4 \text{ km}$ . Compared with the periods of the expected GW signals, that from tens to thousands of seconds, the delay time difference  $\Delta L_{ij}/c \leq 0.08 \text{ s}$  is rather small, and this means that the differences of the extra noises in the above equation will sufficiently suppress noises with correlation times longer than a few

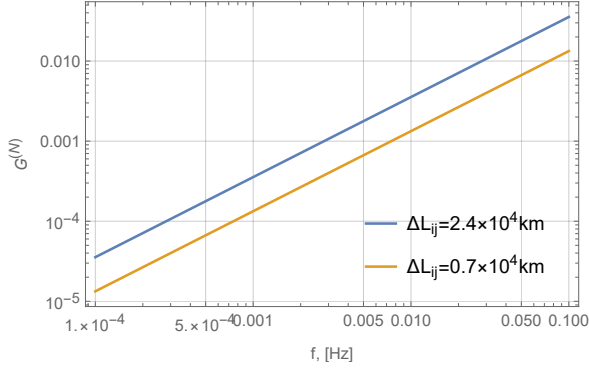


Figure 3: The GRS noise suppression factor for the general TDI combination  $P_i^{(n)}$ .

seconds. In terms of Fourier components, we have

$$\begin{aligned} \mathcal{F}[P_2] = & \frac{(1 - e^{-2\pi i f \frac{\Delta L_{31}}{c}})}{\sqrt{2}} \{ \mathcal{F}[D_3(\vec{n}_3 \cdot \frac{d\vec{\delta}_2^E}{cdt})] \\ & + \mathcal{F}[D_3(\vec{n}_{1'} \cdot \frac{d\vec{\delta}_2^E}{cdt})] + \mathcal{F}[D_3 D_2(\vec{n}_{1'} \cdot \frac{d\vec{\delta}_2^E}{cdt})] \\ & + \mathcal{F}[D_3 D_2(\vec{n}_3 \cdot \frac{d\vec{\delta}_2^E}{cdt})] \} + \frac{1}{\sqrt{2}} \mathcal{F}[N.T.], \quad (8) \end{aligned}$$

where  $\mathcal{F}[\cdot]$  denotes the Fourier transformation. The overall factor  $G = (1 - e^{-2\pi i f \frac{\Delta L_{31}}{c}})/\sqrt{2}$  is the GRS noise suppression factor in Fourier space of the  $P_2$  channel. For the other two channels

$$P_1 = \frac{1}{\sqrt{2}}(\beta + \gamma), \quad P_3 = \frac{1}{\sqrt{2}}(\alpha + \beta),$$

and the derivations are the same.

For the  $N$ th generation case, we define the position noise suppressing channels as

$$P_i^{(N)} = \frac{1}{\sqrt{2}} \sum_{j=1, j \neq i}^3 \alpha_j^{(N)}, \quad (9)$$

where  $\alpha_j^{(N)}$  denotes the  $N$ th generation Sagnac-type TDI combination. With similar algebra and considering realistic cases with  $N \leq 5$ , we derive the GRS noise suppression factor  $G^{(N)}$  for the  $N$ th generation case, see Fig. 3,

$$G_i^{(N)}(f) = \frac{(1 - e^{-2\pi i f \frac{\Delta L_{jk}}{c}})}{\sqrt{2}}, \quad j, k \neq i. \quad (10)$$

This general result is obtained under the condition that during the time  $\tau \sim 30N$  s of one laser loop of the  $N$ th Sagnac combination, the armlength changes  $\delta L_i \leq 180N$  m (relative velocity  $\leq 6$  m/s) which are much smaller compared to the upper bound of the armlength difference,  $\frac{\delta L_i}{\Delta L_{ij}} < 4 \times 10^{-5}$  for  $N \leq 5$ .

We find that, without knowing the details of the noise models, in the mission sensitive band from 0.1 mHz  $\sim$  0.05 Hz, the  $P_i^{(n)}$  channels have the capability to suppress or wipe out the noises from the GRS  $i$  and  $i'$  onboard S/C<sub>*i*</sub> with a factor about  $10^{-5} \sim 10^{-3}$ . This may provide us a new solution to resolve the issues or faults caused by GRS anomalies, and then reduce greatly the relevant risks for the LISA and Taiji missions

## B. Numerical simulations

To demonstrate and confirm the performances of the GRS noise suppression channels  $P_i^{(n)}$ , we carried the numerical simulations for LISA-like missions based on the Taiji simulator package **TaijiSim**. With the modular **TaijiSim-Noise**, we generate the data sets with glitches, continuous disturbances, and their mixes for one or both of the two GRS systems onboard S/C<sub>2</sub>, please see Fig. 4 for illustrations. For realistic use, with the modular **TaijiSim-TDI**, how such

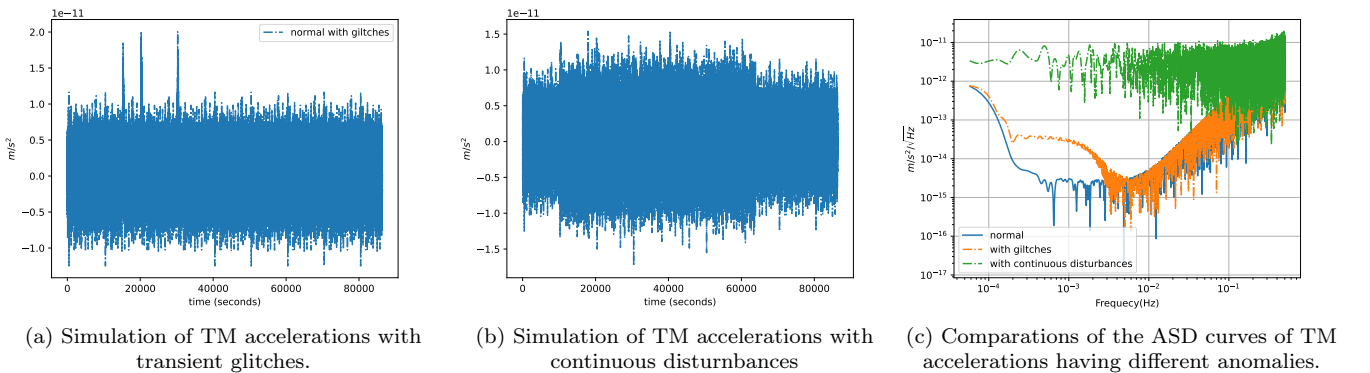


Figure 4: Simulations of TM accelerations having different anomalies.

GRS anomalies will affect the data products from the conventional 2nd generation TDI combinations can be drawn in the ASD curves in Fig. 5a and 5b. As expected, when disturbances took place in both the GRS 2 and 2', such extra noises would heavily pollute the resulted data. The ASD curves of the data from the 2nd generation position noise suppressing

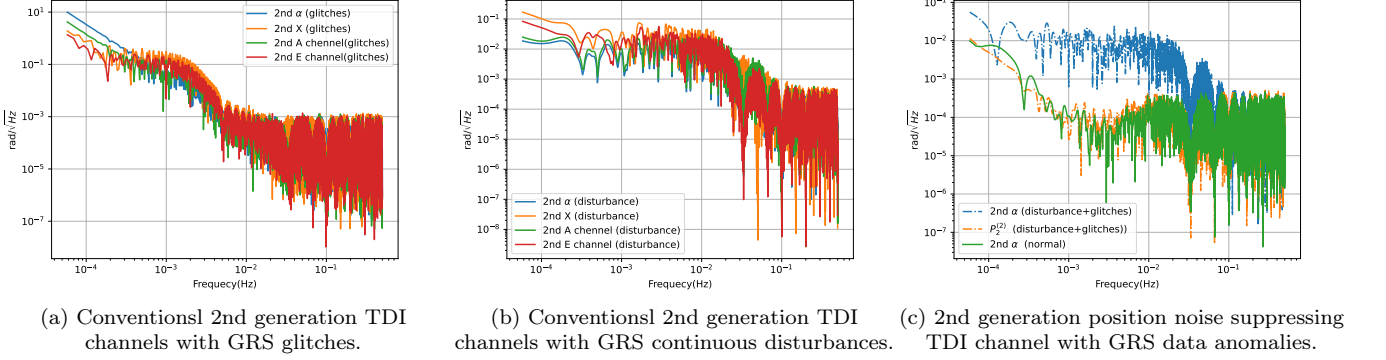


Figure 5: Simulations of 2nd generation TDI channels and the suppression of the GRS anomalies.

suppressing channel  $P_2^{(2)}$  is shown in Fig. 5c, one could see that the extra noises from GRS 2 and 2' are sufficiently reduced in the data (orange curve) and the residual noises return to the expected level for normal cases without data anomalies (green curve). As one could expect, with these channels the effects of the extra GRS disturbances are, in some sense, absent in the final data products, and may have little effect on the science data analysis. In Fig. 6, we consider the cases with only the noise terms from GRS 2 and 2' been included in the simulation, and the efficiencies of the GRS noise suppression by  $P_2$  and  $P_2^{(2)}$  are demonstrated and confirmed, which agree with the analytical result in Eq. (10).

## V. CONCLUDING REMARKS

In this work, we reconsidered the GRS data anomalies caused by disturbances from the surrounding environments or the satellite platforms for the LISA and the LISA-like Taiji missions, which will most likely take place during their science operations. Especially, continuous disturbances to the GRS systems would give rise to the rather long term noisy data and may seriously affect the GW detections in the science data analysis. An even more extreme case is also considered, that one S/C may not retain its ultra stable and clean state and the two measurement arms would be significantly affected by the GRS position noises of that S/C.

To resolve this issues, we suggest the set of TDI channels  $P_i^{(N)}$  ( $i = 1, 2, 3$ ), for realistic considerations the generation  $N \leq 5$ . Without the needs for detailed noise models, such TDI channels could sufficiently suppress the position noises from the GRS  $i$  and  $i'$ . With analytical derivations and numerical simulations, we have proved that the GRS position noise suppression factor could reach  $10^{-5} \sim 10^{-3}$  in the sensitive band  $0.1 \text{ mHz} \sim 0.05 \text{ Hz}$ , given the optimized mission orbits with arm-length changes  $\leq 1.2 \times 10^4 \text{ km}$  and relative velocities  $\leq 6 \text{ m/s}$ . Even for the aforementioned extreme cases, that the GRS noises from one S/C<sub>*i*</sub> grown to 4  $\sim$  5 orders of magnitude larger than the designed level in the

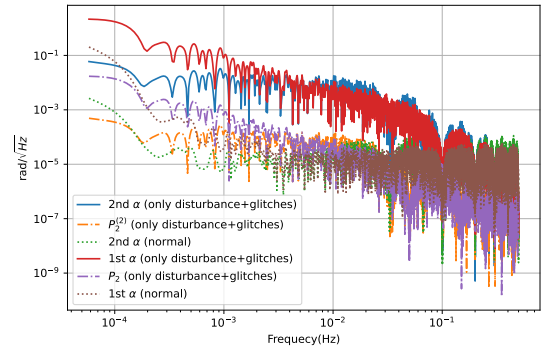


Figure 6: Simulations of the efficiency of the position noise suppression channels.

low frequency band  $\leq 3 \text{ mHz}$ , the channel  $P_i^{(N)}$  could still successfully suppress and wipe out the extra GRS noises and retain the expected sensitivity level for the data.

With this TDI channels, we provide a new solution for the LISA-like missions to resolve the possible issues or faults caused by GRS anomalies. With this approach, the feasibility of the LISA and Taiji missions could be improved, and the risks relate to GRS systems could be significantly reduced.



## ACKNOWLEDGMENTS

This work is supported by the National Key Research and Development Program of China No.

2020YFC2200601 and No. 2021YFC2201901, and the Strategic Priority Research Program of the Chinese Academy of Sciences Grant No. XDA1502110202-02 and No. XDA1502110104-02.

- 
- [1] The LIGO Scientific Collaboration, *Classical and Quantum Gravity* **32**, 074001 (2015).
  - [2] LIGO Scientific Collaboration and Virgo Collaboration, *Physical Review Letters* **116**, 061102 (2016).
  - [3] LIGO Scientific Collaboration and Virgo Collaboration, *Physical Review D* **93**, 122004 (2016).
  - [4] LIGO Scientific Collaboration and Virgo Collaboration, *Physical Review Letters* **116**, 241102 (2016).
  - [5] K. Danzmann and t. L. s. team, *Classical and Quantum Gravity* **13**, A247 (1996).
  - [6] K. D. f. t. L. S. Team, *Classical and Quantum Gravity* **14**, 1399 (1997).
  - [7] K. Danzmann, *Advances in Space Research* **25**, 1129 (2000).
  - [8] K. Danzmann, *LISA Laser Interferometer Space Antenna*, Proposal (2017).
  - [9] P. L. Bender, *Classical and Quantum Gravity* **21**, S1203 (2004).
  - [10] X. Gong, S. Xu, S. Bai, *et al.*, *Classical and Quantum Gravity* **28**, 094012 (2011).
  - [11] X. Gong, Y.-K. Lau, S. Xu, *et al.*, *Journal of Physics: Conference Series* **610**, 012011 (2015).
  - [12] G. Xue-fei, X. Sheng-nian, Y. Ye-fei, *et al.*, *Chinese Astronomy and Astrophysics* **39**, 411 (2015).
  - [13] M. Armano, H. Audley, G. Auger, *et al.*, *Physical Review Letters* **116**, 231101 (2016).
  - [14] M. Armano, H. Audley, J. Baird, *et al.*, *Physical Review Letters* **120** (2018), 10.1103/PhysRevLett.120.061101.
  - [15] M. Armano, arXiv , 1903.08924 (2019).
  - [16] W.-R. Hu and Y.-L. Wu, *National Science Review* **4**, 685 (2017).
  - [17] Z. Luo, Y. Wang, Y. Wu, W. Hu, and G. Jin, *Progress of Theoretical and Experimental Physics* , pta083 (2020).
  - [18] Z. Luo, Z. Guo, G. Jin, Y. Wu, and W. Hu, *Results in Physics* **16**, 102918 (2020).
  - [19] W.-H. Ruan, Z.-K. Guo, R.-G. Cai, and Y.-Z. Zhang, *International Journal of Modern Physics A* **35**, 2050075 (2020).
  - [20] H. Omiya and N. Seto, *Physical Review D* **102**, 084053 (2020).
  - [21] W.-H. Ruan, C. Liu, Z.-K. Guo, Y.-L. Wu, and R.-G. Cai, *Nature Astronomy* **4**, 108 (2020).
  - [22] W.-H. Ruan, C. Liu, Z.-K. Guo, Y.-L. Wu, and R.-G. Cai, *Research* **2021**, 1 (2021).
  - [23] G. Wang, W.-T. Ni, W.-B. Han, P. Xu, and Z. Luo, *Physical Review D* **104**, 024012 (2021).
  - [24] G. Wang and W.-B. Han, *Physical Review D* **103**, 064021 (2021).
  - [25] Q. Baghi, N. Korsakova, J. Slutsky, E. Castelli, N. Karnesis, and J.-B. Bayle, *Physical Review D* **105**, 042002 (2022).
  - [26] B. Frommknecht, *Integrated Sensor Analysis of the GRACE Mission*, Ph.D. thesis, Technische Universität München (2007).
  - [27] The Taiji Scientific Collaboration, *Communications Physics* **4**, 34 (2021).
  - [28] S. E. Pollack, *Classical and Quantum Gravity* **21**, 3419 (2004).
  - [29] J. Carré and E. K. Porter, arXiv:1010.1641 [gr-qc] (2010), arXiv: 1010.1641.
  - [30] Q. Baghi, J. Slutsky, J. I. Thorpe, N. Korsakova, N. Karnesis, and A. Petiteau, , 5 (2018).
  - [31] T. Robson and N. J. Cornish, *Physical Review D* **99**, 024019 (2019).
  - [32] M. C. Edwards, P. Maturana-Russel, R. Meyer, J. Gair, N. Korsakova, and N. Christensen, *Physical Review D* **102**, 084062 (2020).
  - [33] K. Dey, N. Karnesis, A. Toubiana, E. Barausse, N. Korsakova, Q. Baghi, and S. Basak, *Physical Review D* **104**, 044035 (2021).
  - [34] M. Otto, G. Heinzl, and K. Danzmann, *Classical and Quantum Gravity* **29**, 205003 (2012).
  - [35] M. Otto, *Time-Delay Interferometry Simulations for the Laser Interferometer Space Antenna*, Ph. D, der Gottfried Wilhelm Leibniz Universität, Hannover Germany (2015).
  - [36] M. Tinto and S. V. Dhurandhar, *Living Reviews in Relativity* **24**, 1 (2021).
  - [37] J.-B. Bayle, *Simulation and Data Analysis for LISA (Instrumental Modeling, Time-Delay Interferometry, Noise-Reduction Performance Study, and Discrimination of Transient Gravitational Signals)*, Ph.D. thesis, Université de Paris (2021).
  - [38] M. Tinto and J. W. Armstrong, *Physical Review D* **59** (1999), 10.1103/PhysRevD.59.102003.
  - [39] J. W. Armstrong, F. B. Estabrook, and M. Tinto, *The Astrophysical Journal* **527**, 814 (1999).
  - [40] W.-T. Ni, J.-T. Shy, S.-M. Tseng, *et al.* (San Diego, CA, 1997) pp. 105–116.
  - [41] M. O. Hartwig, *Instrumental modelling and noise reduction algorithms for the Laser Interferometer Space Antenna*, Ph.D. thesis, Gottfried Wilhelm Leibniz Universität Hannover (2021).
  - [42] M. Muratore, *Time delay interferometry for LISA science and instrument characterization*, Ph.D. thesis, University of Trento (2021).
  - [43] O. Jennrich, *Classical and Quantum Gravity* **26**, 153001 (2009).
  - [44] N. Peterseim, *TWANGS - High-Frequency Disturbing Signals in 10 Hz Accelerometer Data of the GRACE Satellites*, Ph.D. thesis, Technischen Universität München (2014).
  - [45] J. Flury, S. Bettadpur, and B. D. Tapley, *Advances in Space Research* **42**, 1414 (2008).
  - [46] N. Peterseim, J. Flury, and A. Schlicht, *Advances in Space Research* **49**, 1388 (2012).
  - [47] N. Peterseim, A. Schlicht, J. Flury, and C. Dahle, in *Observation of the System Earth from Space - CHAMP, GRACE, GOCE and future missions*, edited by F. Flechtner, N. Sneeuw, and W.-D. Schuh (Springer

- Berlin Heidelberg, Berlin, Heidelberg, 2014) pp. 53–61, series Title: Advanced Technologies in Earth Sciences.
- [48] The Taiji Scientific Collaboration, International Journal of Modern Physics A **36**, 2102002 (2021).
  - [49] Z. Cai, International Journal of Modern Physics A **36**, 2140020 (2021).
  - [50] J. Min, J.-G. Lei, Y.-P. Li, *et al.*, International Journal of Modern Physics A **36**, 2140011 (2021).
  - [51] X. Peng, H. Jin, P. Xu, *et al.*, International Journal of Modern Physics A **36**, 2140026 (2021).
  - [52] Z. Wang, International Journal of Modern Physics A **36**, 2140008 (2021).
  - [53] M. Muratore, D. Vetrugno, S. Vitale, and O. Hartwig, Physical Review D **105**, 023009 (2022).
  - [54] O. Hartwig and M. Muratore, Physical Review D **105**, 062006 (2022).
  - [55] G. Wang, B. Li, P. Xu, and X. Fan, arXiv:2201.10902 [gr-qc] (2022), arXiv: 2201.10902.
  - [56] D. A. Shaddock, Physical Review D **69** (2004), 10.1103/PhysRevD.69.022001.